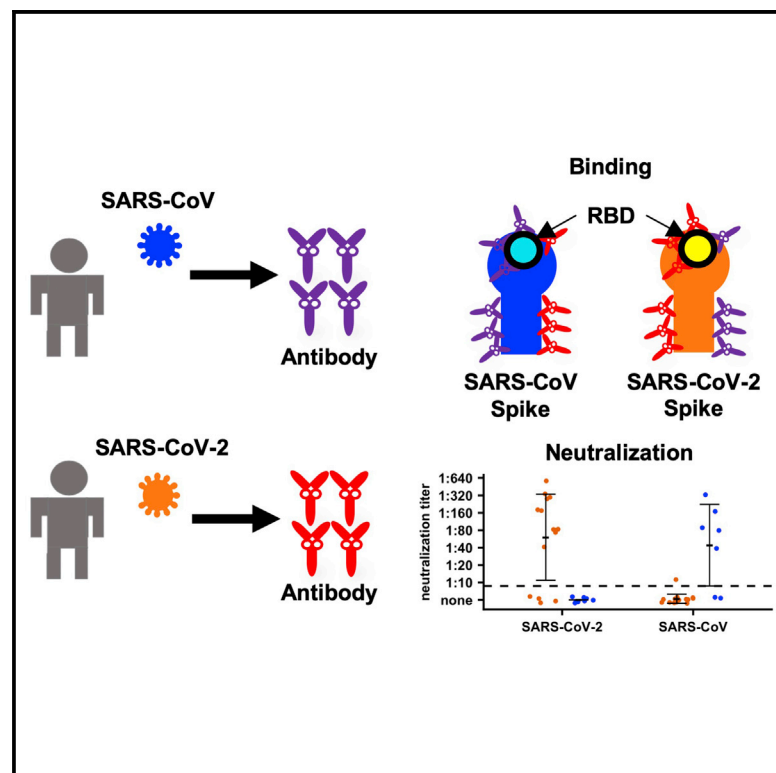# Cross-reactive Antibody Response between SARS-CoV-2 and SARS-CoV Infections

## Graphical Abstract



## Authors

Huibin Lv, Nicholas C. Wu,
Owen Tak-Yin Tsang, ..., J.S. Malik Peiris,
Ian A. Wilson, Chris K.P. Mok

## Correspondence

malik@hku.hk (J.S.M.P.),
wilson@scripps.edu (I.A.W.),
ch02mkp@hku.hk (C.K.P.M.)

## In Brief

Lv et al. examine the antibody responses from patients infected by SARS-CoV-2 or SARS-CoV and from infected or immunized mice. The results show that cross-reactive binding to the spike protein is common, whereas cross-neutralization of the live viruses may be rare.

## Highlights

- Cross-reactive antigen binding is common between SARS-CoV and SARS-CoV-2

- Cross-reactive antibody responses target both RBD and non-RBD regions

- Cross-neutralization of live viruses may be rare between SARS-CoV and SARS-CoV-2

# Cross-reactive Antibody Response
# between SARS-CoV-2 and SARS-CoV Infections

Huibin Lv,[1,7] Nicholas C. Wu,[2,7] Owen Tak-Yin Tsang,[3,7] Meng Yuan,[2] Ranawaka A.P.M. Perera,[4] Wai Shing Leung,[3]
Ray T.Y. So,[1] Jacky Man Chun Chan,[3] Garrick K. Yip,[1] Thomas Shiu Hong Chik,[3] Yiquan Wang,[1] Chris Yau Chung Choi,[3]
Yihan Lin,[1] Wilson W. Ng,[1] Jincun Zhao,[5] Leo L.M. Poon,[1] J.S. Malik Peiris,[1,4,*] Ian A. Wilson,[2,6,*] and Chris K.P. Mok[1,8,*]
[1]HKU-Pasteur Research Pole, School of Public Health, Li Ka Shing Faculty of Medicine, The University of Hong Kong, Hong Kong SAR, China
[2]Department of Integrative Structural and Computational Biology, The Scripps Research Institute, La Jolla, CA 92037, USA
[3]Infectious Diseases Centre, Princess Margaret Hospital, Hospital Authority of Hong Kong, Hong Kong SAR, China
[4]School of Public Health, Li Ka Shing Faculty of Medicine, The University of Hong Kong, Hong Kong SAR, China
[5]State Key Laboratory of Respiratory Disease, National Clinical Research Center for Respiratory Disease, Guangzhou Institute of Respiratory
Health, The First Affiliated Hospital of Guangzhou Medical University, Guangzhou, China
[6]The Skaggs Institute for Chemical Biology, The Scripps Research Institute, La Jolla, CA 92037, USA
[7]These authors contributed equally
[8]Lead Contact
*Correspondence: malik@hku.hk (J.S.M.P.), wilson@scripps.edu (I.A.W.), ch02mkp@hku.hk (C.K.P.M.)
https://doi.org/10.1016/j.celrep.2020.107725

## SUMMARY

The World Health Organization has declared the ongoing outbreak of COVID-19, which is caused by a novel coronavirus SARS-CoV-2, a pandemic. There is currently a lack of knowledge about the antibody response elicited from SARS-CoV-2 infection. One major immunological question concerns antigenic differences between SARS-CoV-2 and SARS-CoV. We address this question by analyzing plasma from patients infected by SARS-CoV-2 or SARS-CoV and from infected or immunized mice. Our results show that, although cross-reactivity in antibody binding to the spike protein is common, cross-neutralization of the live viruses may be rare, indicating the presence of a non-neutralizing antibody response to conserved epitopes in the spike. Whether such low or non-neutralizing antibody response leads to antibody-dependent disease enhancement needs to be addressed in the future. Overall, this study not only addresses a fundamental question regarding antigenicity differences between SARS-CoV-2 and SARS-CoV but also has implications for immunogen design and vaccine development.

## INTRODUCTION

The emergence and spread of a novel coronavirus, SARS-CoV-2, causing severe respiratory disease (COVID-19) has now led to a pandemic with a major impact on global health, the economy, and societal behavior (Poon and Peiris, 2020; Coronaviridae Study Group of the International Committee on Taxonomy of Viruses, 2020; Zhu et al., 2020). By March 15, 2020, more than 150,000 confirmed cases of SARS-CoV-2 had been reported, with close to 6,000 deaths. Now, a month later, those numbers have swelled to 2.4 million cases globally, with more than 165,000 deaths. Phylogenetic analysis has demonstrated that SARS-CoV-2 and SARS-CoV, a coronavirus that also caused a global outbreak in 2003, are closely related phylogenetically, with genomic nucleotide sequence identity of ~80% (Wu et al., 2020; Zhou et al., 2020). Moreover, both viruses use the angiotensin-converting enzyme 2 (ACE2) as the receptor for cell entry and infection (Hoffmann et al., 2020; Letko et al., 2020; Li et al., 2003; Zhou et al., 2020).

The spike glycoprotein (S) on the surface of coronaviruses is essential for virus entry through binding to the ACE2 receptor and for viral fusion with the host cell. The S protein forms a homo-

trimer in which each protomer is composed of two subunits, S1 and S2 (Figure 1A). Binding of the receptor-binding domain (RBD) in the S1 subunit to the ACE2 receptor triggers a conformational change in the S protein that subsequently initiates membrane fusion events with the host cell. The RBD is also a primary target of the antibody response in humoral immunity and is believed to be the major protective antigenic region in SARS-CoV (Chen et al., 2005). The prefusion structure of the S protein of SARS-CoV-2 was recently determined by cryogenic electron microscopy (cryo-EM) (Wrapp et al., 2020) and revealed an overall structural similarity to that of SARS-CoV. However, most monoclonal antibodies tested to date that target the RBD of SARS-CoV have failed to bind to the RBD of SARS-CoV-2 (Tian et al., 2020; Wrapp et al., 2020), suggesting that the antigenicity of these two viruses to the RBD is quite distinct. So far, data have not yet been reported from polyclonal human sera from patients to evaluate the antibody response elicited by SARS-CoV-2 infection and to determine whether cross-reactive antibody responses between SARS-CoV-2 and SARS-CoV can be generated. In this study, we examined the antibody responses in 15 patients from Hong Kong who were infected by SARS-CoV-2, and seven who were infected by SARS-CoV.
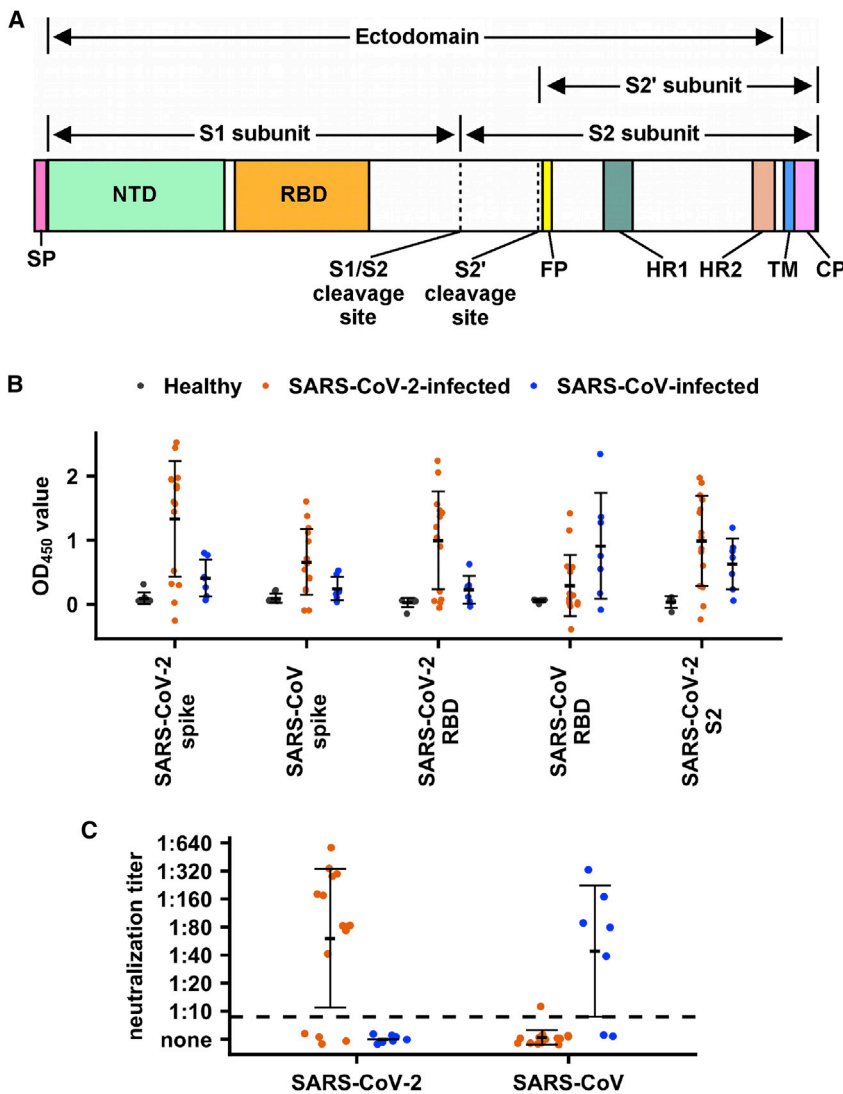
**Figure 1. Human Serological Responses to SARS-CoV-2**

(A) Schematic diagram of the SARS-CoV-2 spike protein. Locations of secretion signal peptide (SP), N-terminal domain (NTD), receptor-binding domain (RBD), S1/S2 cleavage site, S2′ cleavage site, fusion peptide (FP), heptad repeat 1 (HR1), heptad repeat 2 (HR2), transmembrane domain (TM), and cytoplasmic domain (CP) are indicated. Regions corresponding to the S1, S2, S2′ subunits, and ectodomain are also indicated.

(B and C) Binding of plasma from healthy donors and SARS-CoV-2-infected patients to SARS-CoV-2 spike protein, SARS-CoV-2 RBD protein, SARS-CoV-2 S2 subunit, SARS-CoV spike protein, and SARS-CoV RBD protein were measured by ELISA (B). The mean $OD_{450}$ values calculated after testing each plasma sample in triplicate are shown. (C) Neutralization activities of plasma from SARS-CoV-2-infected patients to SARS-CoV-2 and SARS-CoV viruses were measured. Dashed line represents the lower detection limit. Black lines indicate means ± SD. (B and C) Grey, plasma samples from healthy donors; orange, plasma samples from SARS-CoV-2-infected patients; blue, plasma samples from SARS-CoV-infected patients. The value from each dot in the figure was taken by the means of two replicates in the same assay.

geted antibodies. Indeed, conformational rearrangements are required to bind the ACE2 receptor where the RBD adopts an "up," versus a "down," conformation (Gui et al., 2017; Song et al., 2018; Yan et al., 2020). Therefore, in the following results, we avoid making a comparison between the binding signals in S protein ELISA and that in RBD ELISA.

When compared with the plasma from healthy donors, plasma from patients from day 11 post-symptom onward have significant binding to the S ectodomain (p < 2e−16, two-tailed t test) and RBD (p = 2e−13, two-tailed t test) of SARS-CoV-2. The observation that none of the plasma from patients on or before day 11 post-symptom binds to the SARS-CoV-2 S ectodomain and RBD is consistent with a previous study that showed seroconversion in SARS-CoV-2-infected patients can be as late as 14 days after symptom onset (Guo et al., 2020; To et al., 2020). Interestingly, the plasma from SARS-CoV-2-infected patients could also cross-react with the SARS-CoV S ectodomain (p = 8e−06, two-tailed t test) and the SARS-CoV RBD (p = 0.048, two-tailed t test) (Figure 1B). Nevertheless, only five of the samples from the SARS-CoV-2-infected patients (patient nos. 4, 6, 11, 14, and 15) had convincing antibody-binding responses to the SARS-CoV RBD (optical density 450 [$OD_{450}$] > 0.5; Figure 1B; Table S1). However, all samples were collected within 22 days after symptom onset, which is fairly early in the maturation of the humoral immune response, when antibody titers are still increasing (Guo et al., 2020). It is possible that more samples would have detectable cross-reactive binding to the SARS-CoV

Mice infected or immunized with SARS-CoV-2 or SARS-CoV were also used to investigate cross-reactivity of antibody responses between SARS-CoV-2 and SARS-CoV.

## RESULTS

### Patient Samples Show Cross-Reactivity in Binding

Fifteen heparin-anticoagulated plasma samples (from day 2 to 22 after symptom onset) from SARS-CoV-2-infected patients were analyzed (Table S1), with plasma samples from healthy donors collected from the Hong Kong Red Cross as controls. Binding of plasma to the trimeric S ectodomain and monomeric RBD of both SARS-CoV-2 and SARS-CoV (Figure S2; see STAR Methods) was measured by ELISA using anti-immunoglobulin G (anti-IgG) secondary antibodies (Figures 1B and S1). RBD on the trimeric S protein is less exposed than the monomeric RBD, especially when it adopts a "down" conformation (Kirchdoerfer et al., 2018; Walls et al., 2020; Wrapp et al., 2020; Yuan et al., 2017), and may hinder binding of some RBD-tar-

RBD if collected at later time points. In summary, these results indicate that the cross-reactive antibody response to the S protein after SARS-CoV-2 infection targets both RBD and non-RBD regions. Consistent with that observation, reactivity of the plasma from SARS-CoV-2-infected patients could be detected with the S2 subunit of SARS-CoV-2 (p = 2e−4, two-tailed t test; Figure 1B).

We also analyzed seven heparin-anticoagulated, convalescent (3–6 months after infection) plasma samples from SARS-CoV-infected patients. Similar to that observed in plasma samples from SARS-CoV-2-infected patients, cross-reactivity in binding could be detected (Figure 1B). As compared with the plasma from healthy donors, SARS-CoV-infected patients have significant cross-reactivity in binding to the SARS-CoV-2 spike (p = 0.03, two-tailed t test), RBD (p = 0.03, two-tailed t test), and the S2 subunit (p = 0.007, two-tailed t test). These findings show that cross-reactivity in binding is common between SARS-CoV and SARS-CoV-2 infections in both directions. Of note, our recombinant S ectodomains of both SARS-CoV-2 and SARS-CoV contained several mutations to stabilize the prefusion conformation (see STAR Methods), which should not affect most neutralizing epitopes.

### Patient Samples Show Limited Cross-Neutralization
We next tested the neutralization activity of these plasma samples from SARS-CoV-2-infected patients. Except for four plasma samples that came from patients who had fewer than 12 days after symptom onset (patient nos. 1, 2, 9, and 13) with concomitantly low reactivity to both SARS-CoV-2 S ectodomain and RBD (OD$_{450}$ < 0.1), all other plasma samples could neutralize the SARS-CoV-2 virus with titers ranging from 1:40 to 1:640 (Figure 1C; Table S1). However, only one plasma sample could cross-neutralize SARS-CoV, with very low neutralization activity (1:10). In fact, that cross-neutralizing plasma sample had the strongest reactivity in binding against SARS-CoV S ectodomain among all 15 patient samples, although its binding activity against SARS-CoV RBD was not the strongest (Table S1).

Similarly, although five of the seven plasma samples from SARS-CoV-convalescent patients could neutralize SARS-CoV with titers ranging from 1:40 to 1:320, none could cross-neutralize SARS-CoV-2 (Figure 1C). These results show that although cross-reactivity in binding is common between plasma from SARS-CoV-2 and SARS-CoV-infected patients, cross-neutralization activity may be rare.

### Cross-Reactivity in Mouse Infection and Immunization
It is unclear how immune history to corona- and other viruses, which is likely to vary among individuals, influences the antibody response to SARS-CoV-2 and SARS-CoV infection. We, therefore, investigated the cross-reactivity of antibody responses to SARS-CoV-2 and SARS-CoV in mice with no such immune history. Live viruses were inoculated into mice either intranasally (infection) or through intraperitoneal injection with adjuvant (immunization). We have previously shown that intraperitoneal injection of live influenza virus together with adjuvant can induce detectable immune response in mice (Wu et al., 2019). Although SARS-CoV can replicate and elicit antibody response in wild-type mice (Yang et al., 2004), SARS-CoV-2 cannot (Bao et al.,

2020). As a result, intraperitoneal injection of SARS-CoV-2 virus with adjuvant provided an alternative way to study the immune response of SARS-CoV-2 virus in vivo.

The antibody responses of plasma collected from mice infected or immunized with SARS-CoV-2 or SARS-CoV (n = 5 or 6 per experimental and control groups) were analyzed by ELISA. Plasma from mice with mock immunization with a genetically more-distant betacoronavirus, coronavirus OC43-CoV, PBS, or adjuvant was used as the negative controls (Figures 2A–2D). As compared with controls, plasma from mice immunized with SARS-CoV-2 virus had significant binding to its autologous S ectodomain (p < 0.002, two-tailed t test; Figure 2A) and RBD (p < 1e−4, two-tailed t test; Figure 2B). Similarly, plasma from mice immunized with SARS-CoV virus had significant binding to its autologous S ectodomain (p < 2e−7, two-tailed t test; Figure 2C) and RBD (p < 6e−6, two-tailed t test; Figure 2D). In addition, plasma from mice immunized with SARS-CoV S ectodomain could react to its autologous RBD (p < 0.02, two-tailed t test; Figure 2D). However, although plasma from mice infected with SARS-CoV virus could react with its autologous S ectodomain (p < 8e−6, two-tailed t test; Figure 2C) and RBD (p < 2e−5, two-tailed t test; Figure 2D), the reactivity of plasma from mice infected with SARS-CoV-2 virus to its autologous S ectodomain and RBD could not be observed in this assay (p > 0.28, two-tailed t test; Figures 2A and 2B). As expected, an antibody response from SARS-CoV-2-infected wild-type mice was not detected because of the inability of SARS-CoV-2 to replicate in wild-type mice (Bao et al., 2020).

Interestingly, we observed some cross-reactivity of plasma from SARS-CoV-2-immunized mice to both the SARS-CoV S ectodomain (p < 4e−5, two-tailed t test; Figure 2C) and the SARS-CoV RBD (p < 0.006, two-tailed t test; Figure 2D), as well as plasma from SARS-CoV-infected mice to the SARS-CoV-2 S ectodomain (p < 0.005, two-tailed t test; Figure 2A) but not to the RBD. Of note, the absence of detectable binding of plasma from SARS-CoV-infected mice to SARS-CoV-2 RBD (Figure 2B) could be due to the overall weak cross-reactive antibody response to SARS-CoV-2, as indicated by the relatively weak binding to the CoV-2 S ectodomain (OD$_{450}$ ranges from 0.3 to 0.8; Figure 2A). It is possible that binding of plasma from SARS-CoV-infected mice to SARS-CoV-2 RBD would become detectable if the overall antibody response increases. Similarly, the lack of detectable binding of plasma from SARS-CoV-immunized mice to either SARS-CoV-2 S ectodomain or RBD (p > 0.5, two-tailed t test) could be due to the overall low antibody response. Despite the presence of cross-reactivity in binding, cross-neutralization activity was not detected in any of the mouse plasma samples (Figures 2E and 2F), corroborating our findings from human patients.

## DISCUSSION

The work shows that antibody responses in the SARS-CoV-2-infected patient cohort are generated to both S protein and RBD in most patients. Furthermore, cross-reactive antigen binding with SARS-CoV can be detected in those plasma samples as well as in mice studies. Those cross-reactive antibody responses target both the RBD and non-RBD regions. Although higher-sequence
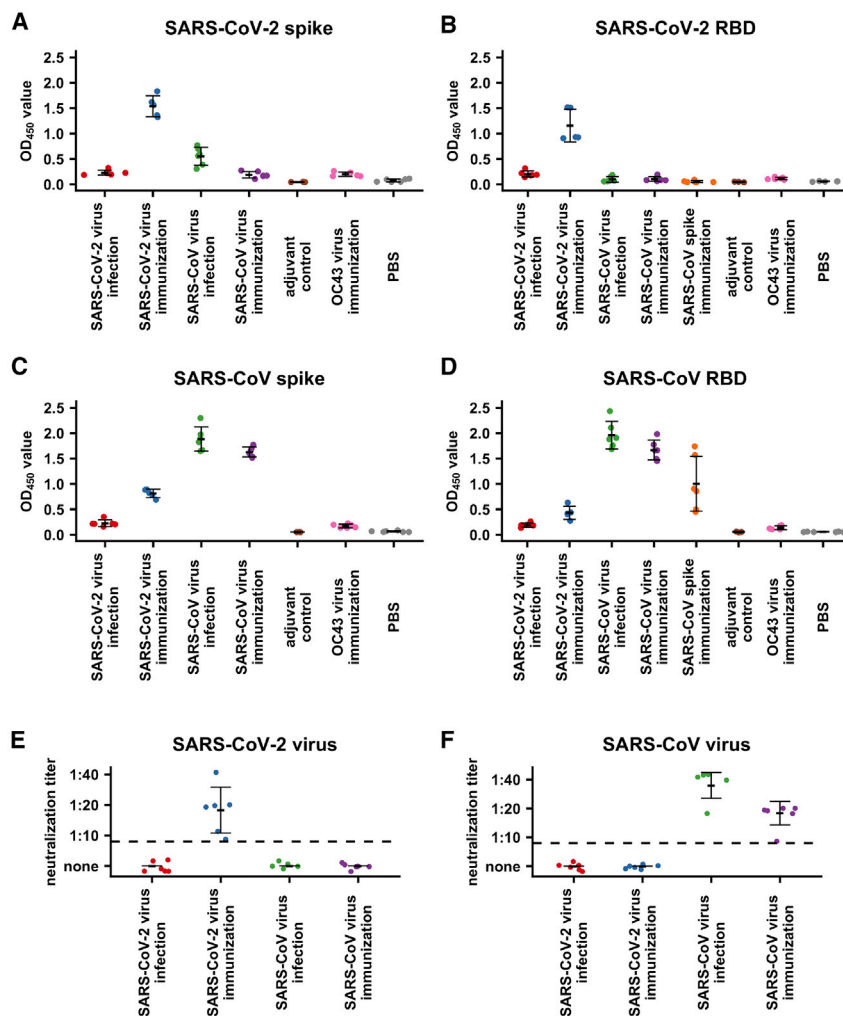
**Figure 2. Mouse Serological Response to SARS-CoV-2 and SARS-CoV**

(A–D) Binding of plasma from OC43-CoV-immunized mice, SARS-CoV-immunized mice, SARS-CoV-infected mice, and mock-immunized mice against (A) SARS-CoV-2 spike protein, (B) SARS-CoV-2 RBD protein, (C) SARS-CoV spike protein, and (D) SARS-CoV RBD protein were measured by ELISA. Because both SARS-CoV spike protein and SARS-CoV-2 spike contained a C-terminal foldon domain, binding of plasma from mice immunized with the SARS-CoV spike protein plasma was not tested against spike proteins from SARS-CoV and SARS-CoV-2. The mean $OD_{450}$ values calculated after testing each plasma sample in triplicate are shown.

(E and F) Neutralization activities of plasma from mice infected or immunized by SARS-CoV-2 or SARS-CoV to (E) SARS-CoV-2 virus or (F) SARS-CoV virus were measured. Dashed line represents the lower detection limit. Black lines indicate means ± SD. The value from each dot in the figure was taken by the means of two replicates in the same assay.

conservation is found between the S2 subunits of SARS-CoV-2 and SARS-CoV (90% amino-acid sequence identity) as compared with that of their RBDs (73% amino-acid sequence identity), some SARS-CoV-2-infected patients were able to produce cross-reactive antibody binding to SARS-CoV RBD. Similarly, a human antibody CR3022 that neutralizes SARS-CoV (ter Meulen et al., 2006) has been reported to also bind to the RBD of SARS-CoV-2 (Tian et al., 2020) by targeting a conserved epitope that is only accessible when at least two RBDs on the trimeric S protein are in the "up" conformation (Yuan et al., 2020). Furthermore, a more recent study has discovered and characterized antibody S309 from memory B cells of a SARS-CoV survivor that cross-neutralizes SARS-CoV and SARS-CoV-2 and targets another conserved epitope that is distinct from the CR3022 epitope (Pinto et al., 2020).

Although cross-reactive antibody-binding responses to both SARS-CoV-2 and SARS-CoV S proteins appear to be relatively common in this cohort, cross-neutralizing responses may be rare. Only one out of 15 SARS-CoV-2-infected patients was able to generate a cross-neutralizing response to both SARS-CoV-2 and SARS-CoV viruses, and that cross-reactive response

was very weak. Therefore, it is possible that only a subset of the cross-reactive binding epitopes is a bona fide neutralizing epitope. This notion is also supported by our recent study, which showed that the cross-reactive antibody CR3022 could not neutralize SARS-CoV-2, despite its relatively strong binding (Yuan et al., 2020). Future studies need to investigate whether these non-neutralizing antibody responses can confer *in vivo* protection despite the lack of *in vitro* neutralization activity (Yuan et al., 2020), which have been observed in some non-neutralizing antibodies to other viruses (Bajic et al., 2019; Bangaru et al., 2019; Bootz et al., 2017; Burke et al., 2018; Dreyfus et al., 2012; Henchal et al., 1988; Lee et al., 2016; Petro et al., 2015; Watanabe et al., 2019). In contrast, non-neutralizing antibody responses can also lead to antibody-dependent enhancement (ADE) of infection as reported in other coronaviruses (Tseng et al., 2012; Wang et al., 2014; Weiss and Scott, 1981). Whether ADE has a role in SARS-CoV-2 infection will need to be carefully examined because of its potential adverse effect in vaccination (Tseng et al., 2012). It will also be important to determine the role of RBD and S2 antibodies, as well as other domains, in neutralization. Competition experiments by preincubating the virus with autologous and heterologous RBD or S2 proteins before incubation with the plasma in neutralization assay may help to further understand mechanisms of cross-reactivity.

SARS-CoV-2 is the third newly emerged coronavirus to cause outbreaks (along with SARS-CoV and MERS-CoV) in the past two decades. Because coronavirus outbreak are likely to continue to pose global health risks in the future (Menachery et al., 2015; Menachery et al., 2016), the possibility of developing

a cross-protective vaccine against multiple coronaviruses has been considered. Identification of cross-protective epitopes on the coronavirus S protein will be important for the development of a more universal coronavirus vaccine analogous to those currently in development for influenza virus (Erbelding et al., 2018; Zost et al., 2019). Our findings, albeit limited at present, would suggest that such broadly cross-neutralizing epitopes to coronaviruses might not be that commonly targeted by the human immune repertoire. Moving forward, monoclonal antibody discovery and characterization will be crucial to development of a SARS-CoV-2 vaccine in the short term as well as a cross-protective coronavirus vaccine in the long term.

## STAR★METHODS

Detailed methods are provided in the online version of this paper and include the following:

- KEY RESOURCES TABLE
- RESOURCE AVAILABILITY
  - Lead contact
  - Materials availability
  - Data and software availability
- EXPERIMENTAL MODEL AND SUBJECT DETAILS
- METHOD DETAILS
  - Collection of plasma samples
  - Protein expression and purification
  - Mouse immunization
  - Mouse infection
  - ELISA binding assay
  - Microneutralization assay
- QUANTIFICATION AND STATISTICAL ANALYSIS

### SUPPLEMENTAL INFORMATION

Supplemental Information can be found online at https://doi.org/10.1016/j.celrep.2020.107725.

### AUTHOR CONTRIBUTIONS

H.L., N.C.W., O.T.-Y.T., J.S.M.P., I.A.W., and C.K.P.M. conceived and designed the study. N.C.W. and M.Y. expressed and purified the proteins. H.L., R.T.Y.S., W.W.N., G.K.Y., Y.L., Y.W., and R.A.P.M.P. performed the experiments. O.T.-Y.T., W.S.L., J.M.C.C., T.S.H.C., and C.Y.C.C. organized patient recruitment, data collection, and sampling. H.L., N.C.W., J.Z., L.L.M.P., and C.K.P.M. analyzed the data. H.L., N.C.W., J.S.M.P., I.A.W., and C.K.P.M. wrote the paper, and all authors reviewed and edited the paper.

### REFERENCES

Bajic, G., Maron, M.J., Adachi, Y., Onodera, T., McCarthy, K.R., McGee, C.E., Sempowski, G.D., Takahashi, Y., Kelsoe, G., Kuraoka, M., and Schmidt, A.G. (2019). Influenza antigen engineering focuses immune responses to a subdominant but broadly protective viral epitope. Cell Host Microbe 25, 827–835.e6.

Bangaru, S., Lang, S., Schotsaert, M., Vanderven, H.A., Zhu, X., Kose, N., Bombardi, R., Finn, J.A., Kent, S.J., Gilchuk, P., et al. (2019). A site of vulnerability on the influenza virus hemagglutinin head domain trimer interface. Cell 177, 1136–1152.e18.

Bao, L., Deng, W., Huang, B., Gao, H., Liu, J., Ren, L., Wei, Q., Yu, P., Xu, Y., Qi, F., et al. (2020). The pathogenicity of SARS-CoV-2 in hACE2 transgenic mice. Nature. https://doi.org/10.1101/2020.02.07.939389.

Bootz, A., Karbach, A., Spindler, J., Kropff, B., Reuter, N., Sticht, H., Winkler, T.H., Britt, W.J., and Mach, M. (2017). Protective capacity of neutralizing and non-neutralizing antibodies against glycoprotein B of cytomegalovirus. PLoS Pathog. 13, e1006601.

Burke, C.W., Froude, J.W., Miethe, S., Hülseweh, B., Hust, M., and Glass, P.J. (2018). Human-like neutralizing antibodies protect mice from aerosol exposure with western equine encephalitis virus. Viruses 10, 147.

Chen, Z., Zhang, L., Qin, C., Ba, L., Yi, C.E., Zhang, F., Wei, Q., He, T., Yu, W., Yu, J., et al. (2005). Recombinant modified vaccinia virus Ankara expressing the spike glycoprotein of severe acute respiratory syndrome coronavirus induces protective neutralizing antibodies primarily targeting the receptor binding region. J. Virol. 79, 2678–2688.

Dreyfus, C., Laursen, N.S., Kwaks, T., Zuijdgeest, D., Khayat, R., Ekiert, D.C., Lee, J.H., Metlagel, Z., Bujny, M.V., Jongeneelen, M., et al. (2012). Highly conserved protective epitopes on influenza B viruses. Science 337, 1343–1348.

Ekiert, D.C., Friesen, R.H., Bhabha, G., Kwaks, T., Jongeneelen, M., Yu, W., Ophorst, C., Cox, F., Korse, H.J., Brandenburg, B., et al. (2011). A highly conserved neutralizing epitope on group 2 influenza A viruses. Science 333, 843–850.

Erbelding, E.J., Post, D.J., Stemmy, E.J., Roberts, P.C., Augustine, A.D., Ferguson, S., Paules, C.I., Graham, B.S., and Fauci, A.S. (2018). A universal influenza vaccine: the strategic plan for the National Institute of Allergy and Infectious Diseases. J. Infect. Dis. 218, 347–354.

Gui, M., Song, W., Zhou, H., Xu, J., Chen, S., Xiang, Y., and Wang, X. (2017). Cryo-electron microscopy structures of the SARS-CoV spike glycoprotein reveal a prerequisite conformational state for receptor binding. Cell Res. 27, 119–129.

Guo, L., Ren, L., Yang, S., Xiao, M., Chang, D., Yang, F., Dela Cruz, C.S., Wang, Y., Wu, C., Xiao, Y., et al. (2020). Profiling early humoral response to diagnose novel coronavirus disease (COVID-19). Clin. Infect. Dis., ciaa310.

Henchal, E.A., Henchal, L.S., and Schlesinger, J.J. (1988). Synergistic interactions of anti-NS1 monoclonal antibodies protect passively immunized mice from lethal challenge with dengue 2 virus. J. Gen. Virol. 69, 2101–2107.

Hoffmann, M., Kleine-Weber, H., Schroeder, S., Krüger, N., Herrler, T., Erichsen, S., Schiergens, T.S., Herrler, G., Wu, N.H., Nitsche, A., et al. (2020). SARS-

CoV-2 cell entry depends on ACE2 and TMPRSS2 and is blocked by a clinically proven protease inhibitor. Cell 181, 271–280.e8.

Kirchdoerfer, R.N., Cottrell, C.A., Wang, N., Pallesen, J., Yassine, H.M., Turner, H.L., Corbett, K.S., Graham, B.S., McLellan, J.S., and Ward, A.B. (2016). Pre-fusion structure of a human coronavirus spike protein. Nature 531, 118–121.

Kirchdoerfer, R.N., Wang, N., Pallesen, J., Wrapp, D., Turner, H.L., Cottrell, C.A., Corbett, K.S., Graham, B.S., McLellan, J.S., and Ward, A.B. (2018). Stabilized coronavirus spikes are resistant to conformational changes induced by receptor recognition or proteolysis. Sci. Rep. 8, 15701.

Lee, J., Boutz, D.R., Chromikova, V., Joyce, M.G., Vollmers, C., Leung, K., Horton, A.P., DeKosky, B.J., Lee, C.H., Lavinder, J.J., et al. (2016). Molecular-level analysis of the serum antibody repertoire in young adults before and after seasonal influenza vaccination. Nat. Med. 22, 1456–1464.

Letko, M., Marzi, A., and Munster, V. (2020). Functional assessment of cell entry and receptor usage for SARS-CoV-2 and other lineage B betacoronaviruses. Nat. Microbiol. 5, 562–569.

Li, W., Moore, M.J., Vasilieva, N., Sui, J., Wong, S.K., Berne, M.A., Somasundaran, M., Sullivan, J.L., Luzuriaga, K., Greenough, T.C., et al. (2003). Angiotensin-converting enzyme 2 is a functional receptor for the SARS coronavirus. Nature 426, 450–454.

Menachery, V.D., Yount, B.L., Jr., Debbink, K., Agnihothram, S., Gralinski, L.E., Plante, J.A., Graham, R.L., Scobey, T., Ge, X.Y., Donaldson, E.F., et al. (2015). A SARS-like cluster of circulating bat coronaviruses shows potential for human emergence. Nat. Med. 21, 1508–1513.

Menachery, V.D., Yount, B.L., Jr., Sims, A.C., Debbink, K., Agnihothram, S.S., Gralinski, L.E., Graham, R.L., Scobey, T., Plante, J.A., Royal, S.R., et al. (2016). SARS-like WIV1-CoV poised for human emergence. Proc. Natl. Acad. Sci. USA 113, 3048–3053.

Moritz, C.P., Tholance, Y., Lassablière, F., Camdessanché, J.P., and Antoine, J.C. (2019). Reducing the risk of misdiagnosis of indirect ELISA by normalizing serum-specific background noise: The example of detecting anti-FGFR3 autoantibodies. J. Immunol. Methods 466, 52–56.

Petro, C., González, P.A., Cheshenko, N., Jandl, T., Khajoueinejad, N., Bénard, A., Sengupta, M., Herold, B.C., and Jacobs, W.R. (2015). Herpes simplex type 2 virus deleted in glycoprotein D protects against vaginal, skin and neural disease. eLife 4, e06054.

Pinto, D., Park, Y.-J., Beltramello, M., Walls, A.C., Tortorici, M.A., Bianchi, S., Jaconi, S., Culap, K., Zatta, F., De Marco, A., et al. (2020). Structural and functional analysis of a potent sarbecovirus neutralizing antibody. bioRxiv. https://doi.org/10.1101/2020.04.07.023903.

Poon, L.L.M., and Peiris, M. (2020). Emergence of a novel human coronavirus threatening human health. Nat. Med. 26, 317–319.

Song, W., Gui, M., Wang, X., and Xiang, Y. (2018). Cryo-EM structure of the SARS coronavirus spike glycoprotein in complex with its host cell receptor ACE2. PLoS Pathog. 14, e1007236.

ter Meulen, J., van den Brink, E.N., Poon, L.L., Marissen, W.E., Leung, C.S., Cox, F., Cheung, C.Y., Bakker, A.Q., Bogaards, J.A., van Deventer, E., et al. (2006). Human monoclonal antibody combination against SARS coronavirus: synergy and coverage of escape mutants. PLoS Med. 3, e237.

Tian, X., Li, C., Huang, A., Xia, S., Lu, S., Shi, Z., Lu, L., Jiang, S., Yang, Z., Wu, Y., and Ying, T. (2020). Potent binding of 2019 novel coronavirus spike protein by a SARS coronavirus-specific human monoclonal antibody. Emerg. Microbes Infect. 9, 382–385.

To, K.K., Tsang, O.T., Leung, W.S., Tam, A.R., Wu, T.C., Lung, D.C., Yip, C.C., Cai, J.P., Chan, J.M., Chik, T.S., et al. (2020). Temporal profiles of viral load in posterior oropharyngeal saliva samples and serum antibody responses during infection by SARS-CoV-2: an observational cohort study. Lancet Infect. Dis. 20, 565–574.

Tseng, C.T., Sbrana, E., Iwata-Yoshikawa, N., Newman, P.C., Garron, T., Atmar, R.L., Peters, C.J., and Couch, R.B. (2012). Immunization with SARS co-ronavirus vaccines leads to pulmonary immunopathology on challenge with the SARS virus. PLoS ONE 7, e35421.

Coronaviridae Study Group of the International Committee on Taxonomy of Viruses (2020). The species Severe acute respiratory syndrome-related coronavirus: classifying 2019-nCoV and naming it SARS-CoV-2. Nat. Microbiol. 5, 536–544.

Walls, A., Tortorici, M.A., Bosch, B.J., Frenz, B., Rottier, P.J., DiMaio, F., Rey, F.A., and Veesler, D. (2017). Crucial steps in the structure determination of a coronavirus spike glycoprotein using cryo-electron microscopy. Protein Sci. 26, 113–121.

Walls, A.C., Park, Y.J., Tortorici, M.A., Wall, A., McGuire, A.T., and Veesler, D. (2020). Structure, function, and antigenicity of the SARS-CoV-2 spike glycoprotein. Cell 181, 281–292.e6.

Wang, S.F., Tseng, S.P., Yen, C.H., Yang, J.Y., Tsao, C.H., Shen, C.W., Chen, K.H., Liu, F.T., Liu, W.T., Chen, Y.M., and Huang, J.C. (2014). Antibody-dependent SARS coronavirus infection is mediated by antibodies against spike proteins. Biochem. Biophys. Res. Commun. 451, 208–214.

Watanabe, A., McCarthy, K.R., Kuraoka, M., Schmidt, A.G., Adachi, Y., Onodera, T., Tonouchi, K., Caradonna, T.M., Bajic, G., Song, S., et al. (2019). Antibodies to a conserved influenza head interface epitope protect by an IgG subtype-dependent mechanism. Cell 177, 1124–1135.e16.

Weiss, R.C., and Scott, F.W. (1981). Antibody-mediated enhancement of disease in feline infectious peritonitis: comparisons with dengue hemorrhagic fever. Comp. Immunol. Microbiol. Infect. Dis. 4, 175–189.

Wong, M.C., Javornik Cregeen, S.J., Ajami, N.J., and Petrosino, J.F. (2020). Evidence of recombination in coronaviruses implicating pangolin origins of nCoV-2019. bioRxiv. https://doi.org/10.1101/2020.02.07.939207.

Wrapp, D., Wang, N., Corbett, K.S., Goldsmith, J.A., Hsieh, C.L., Abiona, O., Graham, B.S., and McLellan, J.S. (2020). Cryo-EM structure of the 2019-nCoV spike in the prefusion conformation. Science 367, 1260–1263.

Wu, N.C., Lv, H., Thompson, A.J., Wu, D.C., Ng, W.W.S., Kadam, R.U., Lin, C.W., Nycholat, C.M., McBride, R., Liang, W., et al. (2019). Preventing an antigenically disruptive mutation in egg-based H3N2 seasonal influenza vaccines by mutational incompatibility. Cell Host Microbe 25, 836–844.e5.

Wu, F., Zhao, S., Yu, B., Chen, Y.M., Wang, W., Song, Z.G., Hu, Y., Tao, Z.W., Tian, J.H., Pei, Y.Y., et al. (2020). A new coronavirus associated with human respiratory disease in China. Nature 579, 265–269.

Yan, R., Zhang, Y., Li, Y., Xia, L., Guo, Y., and Zhou, Q. (2020). Structural basis for the recognition of SARS-CoV-2 by full-length human ACE2. Science 367, 1444–1448.

Yang, Z.Y., Kong, W.P., Huang, Y., Roberts, A., Murphy, B.R., Subbarao, K., and Nabel, G.J. (2004). A DNA vaccine induces SARS coronavirus neutralization and protective immunity in mice. Nature 428, 561–564.

Yuan, Y., Cao, D., Zhang, Y., Ma, J., Qi, J., Wang, Q., Lu, G., Wu, Y., Yan, J., Shi, Y., et al. (2017). Cryo-EM structures of MERS-CoV and SARS-CoV spike glycoproteins reveal the dynamic receptor binding domains. Nat. Commun. 8, 15092.

Yuan, M., Wu, N.C., Zhu, X., Lee, C.D., So, R.T.Y., Lv, H., Mok, C.K.P., and Wilson, I.A. (2020). A highly conserved cryptic epitope in the receptor binding domains of SARS-CoV-2 and SARS-CoV. Science 368, 630–633.

Zhou, P., Yang, X.L., Wang, X.G., Hu, B., Zhang, L., Zhang, W., Si, H.R., Zhu, Y., Li, B., Huang, C.L., et al. (2020). A pneumonia outbreak associated with a new coronavirus of probable bat origin. Nature 579, 270–273.

Zhu, N., Zhang, D., Wang, W., Li, X., Yang, B., Song, J., Zhao, X., Huang, B., Shi, W., Lu, R., et al.; China Novel Coronavirus Investigating and Research Team (2020). A novel coronavirus from patients with pneumonia in China, 2019. N. Engl. J. Med. 382, 727–733.

Zost, S.J., Wu, N.C., Hensley, S.E., and Wilson, I.A. (2019). Immunodominance and antigenic variation of influenza virus hemagglutinin: implications for design of universal vaccine immunogens. J. Infect. Dis. 219 (Suppl_1), S38–S45.

## STAR★METHODS

### KEY RESOURCES TABLE

| REAGENT or RESOURCE | SOURCE | IDENTIFIER |
| --- | --- | --- |
| **Biological Samples** | | |
| Plasma from SARS-CoV-2 patients | Hospital Authority of Hong Kong | N/A |
| Plasma from SARS-CoV survivors | Hospital Authority of Hong Kong | N/A |
| Plasma from healthy donors | Hong Kong Red Cross | N/A |
| **Chemicals and Recombinant Proteins** | | |
| S2 extracellular domain of SARS-CoV-2 | Sino Biological | 40590-V08B |
| DpnI | New England Biolabs | R0176L |
| Trypsin | New England Biolabs | P8101S |
| PBS | Corning | 21-040-CMR |
| Bovine Serum Albumin (BSA) | Sigma-Aldrich | A9418 |
| Tween 20 | Fisher Scientific | BP337-500 |
| AMDEX sheep anti-human IgG-HRP | GE Healthcare | RPN4101 |
| AMDEX sheep anti-mouse IgG-HRP | GE Healthcare | RPN4201 |
| Ketamine | Alfasan International BV | 1711347-09 |
| Xylazine | Alfasan International BV | 1804117-11 |
| **Critical Commercial Assays** | | |
| In-Fusion HD Cloning Kit | Takara | 639647 |
| KOD Hot Start DNA Polymerase | EMD Millipore | 71086-3 |
| PCR Clean-Up and Gel Extraction Kit | Clontech Laboratories | 740609.250 |
| QIAprep Spin Miniprep Kit | QIAGEN | 27106 |
| **Cell Lines** | | |
| Sf9 cells | ATCC | CRL-1711 |
| High Five cells | Thermo Fisher Scientific | B85502 |
| Vero cells | ATCC | CCL-81 |
| Vero E6 cells | ATCC | CCL-1586 |
| **Deposited Data** | | |
| SARS-CoV-2 spike protein sequence | NCBI Reference Sequence | YP_009724390.1 |
| SARS-CoV spike protein sequence | GenBank | ABF65836.1 |
| **Oligonucleotides** | | |
| Primers for cloning | Integrated DNA Technologies | N/A |
| **Recombinant DNA** | | |
| pFastBac-SARS-CoV-2 spike ectodomain | This study | N/A |
| pFastBac-SARS-CoV spike ectodomain | This study | N/A |
| pFastBac-SARS-CoV-2 RBD | This study | N/A |
| pFastBac-SARS-CoV RBD | This study | N/A |
| **Software and Algorithms** | | |
| R | https://www.r-project.org | N/A |
| **Other** | | |
| HyClone insect cell culture medium | GE Healthcare | SH30280.03 |
| DMEM | Thermo Fisher Scientific | 11965-092 |
| Addavax | InvivoGen | vac-adx-10 |
| Nunc MaxiSorp ELISA plate | Nunc MaxiSorp ELISA plate | 44-2404-21 |
| Phosphate-buffered saline (PBS) | Thermo Fisher Scientific | 14040133 |

| *Continued* | | |
| --- | --- | --- |
| REAGENT or RESOURCE | SOURCE | IDENTIFIER |
| Ni-NTA Superflow | QIAGEN | 30450 |
| FuGENE HD | Promega | E2311 |
| DH10Bac competent cells | Thermo Fisher Scientific | 10361012 |

## RESOURCE AVAILABILITY

### Lead contact
Further information and requests for resources and reagents should be directed to and will be fulfilled by the Lead Contact, Chris K. P. Mok (ch02mkp@hku.hk).

### Materials availability
All unique/stable reagents generated in this study are available from the Lead Contact with a completed Materials Transfer Agreement.

### Data and software availability
This study did not generate any unique datasets or code.

## EXPERIMENTAL MODEL AND SUBJECT DETAILS

Vero and Vero E6 cells were maintained in DMEM medium supplemented with 10% fetal bovine serum (FBS), and 100 U mL$^{-1}$ of Penicillin-Streptomycin. Sf9 cells (*Spodoptera frugiperda* ovarian cells, female) and High Five cells (*Trichoplusia ni* ovarian cells, female) were maintained in HyClone insect cell culture medium.

Patient-derived SARS-CoV-2 (BetaCoV/Hong Kong/VM20001061/2020 [KH1]) and SARS-CoV (strain HK39849, SCoV) were passaged in Vero-E6 cells and the virus stock was aliquoted and titrated to determine tissue culture infection dose 50% (TCID$_{50}$) in Vero-E6 cells. The neutralization experiments were carried out in a Bio-safety level 3 (BSL-3) facility at the School of Public Health, LKS Faculty of Medicine, The University of Hong Kong.

Patients with RT-PCR confirmed COVID-19 disease at the Infectious Disease Centre of the Princess Margaret Hospital, Hong Kong, were invited to participate in the study after providing informed consent. The age and gender of the patients are listed in Table S1. The study was approved by the institutional review board of the Hong Kong West Cluster of the Hospital Authority of Hong Kong (approval number: UW20-169). 6-8 weeks old male BALB/c mice were used in this study. The experiments were conducted in The University of Hong Kong Biosafety Level 3 (BSL3) facility. The study protocol was carried out in strict accordance with the recommendations and was approved by the Committee on the Use of Live Animals in Teaching and Research of the University of Hong Kong (CULATR 4533-17).

## METHOD DETAILS

### Collection of plasma samples
Specimens of heparinized blood were collected from the patients, and the plasma were separated and stored at −80°C until use. The plasma was heat inactivated at 56°C for 30 minutes before use. The plasma samples from patients with SARS-CoV infection were obtained from the bio-repository of specimens stored from patients following the SARS outbreak in 2003.

### Protein expression and purification
Ectodomain (residues 14-1195) with K968P/V969P mutations and RBD (residues: 306-527) of the SARS-CoV spike (S) protein (GenBank: ABF65836.1), as well as the ectodomain (residues 14-1213) with R682G/R683G/R685G/K986P/V987P mutations and RBD (residues 319-541) of the SARS-CoV-2 spike protein (GenBank: QHD43416.1) were cloned into a customized pFastBac vector (Ekiert et al., 2011). K968P/V969P were stabilizing mutations inserted into the SARS-CoV spike protein (Kirchdoerfer et al., 2018) and the corresponding K986P/V987P mutations in the SARS-CoV-2 spike protein were intended to have the same stabilizing effect due to sequence similarity. R682G/R683G/R685G mutations in the SARS-CoV-2 spike protein were designed to knock-out the furin cleavage site that is a novel addition to this particular coronavirus compared to related sequences in bats and pangolins, as well as other coronaviruses (Wong et al., 2020). Furin cleavage site knockout mutations can stabilize the prefusion conformation of the coronavirus spike ectodomain by preventing furin processing without affecting its overall structure (Kirchdoerfer et al., 2016; Walls et al., 2017). In fact, both K986P/V987P mutations and furin cleavage site knockout mutations were present in the recent recombinant SARS-CoV-2 spike ectodomain constructs (Walls et al., 2020; Wrapp et al., 2020). The spike ectodomain constructs were fused with an N-terminal gp67 signal peptide and a C-terminal BirA biotinylation site, thrombin cleavage site, trimerization domain, and His$_6$ tag.

The RBD constructs were fused with an N-terminal gp67 signal peptide and a C-terminal His$_6$ tag. Recombinant bacmid DNA was generated using the Bac-to-Bac system (Life Technologies). Baculovirus was generated by transfecting purified bacmid DNA into Sf9 cells using FuGENE HD (Promega), and subsequently used to infect suspension cultures of High Five cells (Life Technologies) at an MOI of 5 to 10. Infected High Five cells were incubated at 28 °C with shaking at 110 rpm for 72 h for protein expression. The supernatant was then concentrated using a Centramate cassette (10 kDa MW cutoff for RBD and 30 kDa MW cutoff for spike protein, Pall Corporation). Spike ectodomain and RBD proteins were purified by Ni-NTA (Figure S2), followed by size exclusion chromatography, and then buffer exchanged into PBS. The S2 extracellular domain of SARS-CoV-2 was purchased from Sino Biological, China.

### Mouse immunization
The BALB/c mice were immunized with $10^5$ pfu of SARS-CoV, SARS-CoV-2, HCoV-OC43 or 15 μg of SARS-CoV spike protein in 150 μL PBS together with 50 μL Addavax (MF59-like squalene adjuvant from InvivoGen) through intraperitoneally injection (i.p.). For the control group, BALB/c mice were injected intraperitoneally (i.p.) with 50 μL Addavax plus 150 μL PBS, or 200 μL PBS only. The plasma samples were collected on day 14 post-vaccination using heparin tubes.

### Mouse infection
6-8 weeks BALB/c mice were anesthetized with Ketamine and Xylazine, and infected intranasally (i.n.) with $10^5$ pfu of patient-derived SARS-CoV or SARS-CoV-2 diluted in 25 μL PBS. Mouse plasma samples were collected on day 14 post-infection using heparin tubes. The experiments were conducted in the University of Hong Kong Biosafety Level 3 (BSL3) facility.

### ELISA binding assay
A 96-well enzyme-linked immunosorbent assay (ELISA) plate (Nunc MaxiSorp, Thermo Fisher Scientific) was first coated overnight with 100 ng per well of purified recombinant protein in PBS buffer. To substrate the background noise caused by the unspecific binding of antibodies from the samples, serum-specific background noise (SSBN) normalization approach was used (Moritz et al., 2019). In brief, an additional plate was coated overnight with PBS buffer only. The plates coated with either purified recombinant protein or PBS were then blocked with PBS containing 5% non-fat milk powder at room temperature for 2 hours. Each mouse plasma sample was 1:10 diluted and human sample was serially diluted from 1:100 to 1:12800 in PBS. Each sample was then added into the ELISA plates that were coated with purified recombinant protein or PBS buffer respectively for 2-hour incubation at 37°C. After extensive washing with PBS containing 0.1% Tween 20, each well in the plate was further incubated with the HRP-sheep anti-mouse IgG or anti-human IgG secondary antibody (1:5000, GE Healthcare) for 1 hour at 37°C. The ELISA plates were then washed five times with PBS containing 0.1% Tween 20. Subsequently, 50 μL of each solution A and B (R&D Systems) was added into each well. After 15 minutes incubation, the reaction was stopped by adding 50 μL of 2 M H$_2$SO$_4$ solution and analyzed on a Sunrise (Tecan) absorbance microplate reader at 450 nm wavelength. The normalized results were obtained by calculating the difference between the OD of the purified recombinant protein-coated well and the PBS-coated well.

### Microneutralization assay
Plasma samples were diluted in serial two-fold dilutions commencing with a dilution of 1:10, and mixed with equal volumes of SARS-CoV or SARS-CoV-2 at a dose of 200 tissue culture infective doses 50% (TCID$_{50}$) determined by Vero and Vero E6 cells respectively. After 1 h of incubation at 37°C, 35 μL of the virus-serum mixture was added in quadruplicate to Vero or Vero E6 cell monolayers in 96-well microtiter plates. After 1 h of adsorption, the virus-serum mixture was removed and replaced with 150ul of virus growth medium in each well. The plates were incubated for 3 days at 37°C in 5% CO$_2$ in a humidified incubator. Cytopathic effect was observed at day 3 post-inoculation. The highest plasma dilution protecting 50% of the replicate wells was denoted as the neutralizing antibody titer. A virus back-titration of the input virus was included in each batch of tests.

### QUANTIFICATION AND STATISTICAL ANALYSIS

The p values reported were computed by the paired Student's t test using the R software package.

# Supplemental Information

# Cross-reactive Antibody Response

# between SARS-CoV-2 and SARS-CoV Infections

**Huibin Lv, Nicholas C. Wu, Owen Tak-Yin Tsang, Meng Yuan, Ranawaka A.P.M. Perera, Wai Shing Leung, Ray T.Y. So, Jacky Man Chun Chan, Garrick K. Yip, Thomas Shiu Hong Chik, Yiquan Wang, Chris Yau Chung Choi, Yihan Lin, Wilson W. Ng, Jincun Zhao, Leo L.M. Poon, J.S. Malik Peiris, Ian A. Wilson, and Chris K.P. Mok**

**Table S1. Patient information, ELISA data, and neutralization data. Related to Figure 1.**

| ID | Gender | Age | day post-symptom onset | ELISA (OD$_{450}$ value at 1:100 dilution) | | | | MN titer | |
| --- | --- | --- | --- | --- | --- | --- | --- | --- | --- |
| | | | | SARS-CoV-2 spike | SARS-CoV spike | SARS-CoV-2 RBD | SARS-CoV RBD | SARS-CoV-2 | SARS-CoV |
| SARS-CoV-2 patient #1 | M | 56 | 6 | 0.30 | 0.21 | 0.03 | 0.01 | <1:10 | <1:10 |
| SARS-CoV-2 patient #2 | F | 62 | 4 | 0.32 | 0.23 | 0.07 | 0.03 | <1:10 | <1:10 |
| SARS-CoV-2 patient #3 | F | 62 | 22 | 1.97 | 0.66 | 1.46 | 0.12 | 1:160 | <1:10 |
| SARS-CoV-2 patient #4 | M | 63 | 22 | 1.95 | 0.98 | 1.56 | 0.58 | 1:80 | <1:10 |
| SARS-CoV-2 patient #5 | M | 47 | 8 | 0.52 | 0.40 | 0.20 | 0.03 | 1:80 | <1:10 |
| SARS-CoV-2 patient #6 | M | 64 | 19 | 1.81 | 0.54 | 1.40 | 0.50 | 1:320 | <1:10 |
| SARS-CoV-2 patient #7 | F | 73 | 18 | 1.60 | 0.71 | 0.90 | 0.17 | 1:80 | <1:10 |
| SARS-CoV-2 patient #8 | M | 72 | 18 | 1.94 | 1.19 | 1.21 | 0.14 | 1:80 | <1:10 |
| SARS-CoV-2 patient #9 | F | 37 | 2 | -0.25 | -0.10 | -0.05 | -0.39 | <1:10 | <1:10 |
| SARS-CoV-2 patient #10 | F | 72 | 10 | 1.44 | 0.41 | 1.04 | -0.03 | 1:40 | <1:10 |
| SARS-CoV-2 patient #11 | M | 60 | 22 | 2.53 | 1.38 | 2.24 | 1.15 | 1:160 | <1:10 |
| SARS-CoV-2 patient #12 | M | 56 | 13 | 1.57 | 0.64 | 1.37 | 0.00 | 1:320 | <1:10 |
| SARS-CoV-2 patient #13 | F | 55 | 11 | 0.03 | -0.09 | 0.05 | 0.08 | <1:10 | <1:10 |
| SARS-CoV-2 patient #14 | F | 63 | 19 | 2.44 | 1.12 | 2.06 | 1.42 | 1:640 | <1:10 |
| SARS-CoV-2 patient #15 | M | 37 | 14 | 1.85 | 1.60 | 1.43 | 0.59 | 1:320 | 1:10 |
| SARS-CoV patient #1 | NA | NA | NA | 0.41 | 0.53 | 0.28 | 0.55 | <1:10 | 1:80 |
| SARS-CoV patient #2 | NA | NA | NA | 0.80 | 0.20 | 0.30 | 1.28 | <1:10 | 1:40 |
| SARS-CoV patient #3 | NA | NA | NA | 0.27 | 0.22 | 0.12 | 0.76 | <1:10 | 1:80 |
| SARS-CoV patient #4 | NA | NA | NA | 0.07 | 0.04 | -0.03 | -0.08 | <1:10 | <1:10 |
| SARS-CoV patient #5 | NA | NA | NA | 0.13 | 0.11 | 0.04 | 0.17 | <1:10 | <1:10 |
| SARS-CoV patient #6 | NA | NA | NA | 0.43 | 0.16 | 0.25 | 1.36 | <1:10 | 1:160 |
| SARS-CoV patient #7 | NA | NA | NA | 0.77 | 0.47 | 0.63 | 2.34 | <1:10 | 1:320 |
| Healthy donor #1 | NA | NA | NA | 0.31 | 0.22 | 0.05 | 0.06 | ND | ND |
| Healthy donor #2 | NA | NA | NA | 0.11 | 0.20 | -0.15 | 0.00 | ND | ND |
| Healthy donor #3 | NA | NA | NA | 0.06 | 0.06 | 0.07 | 0.07 | ND | ND |
| Healthy donor #4 | NA | NA | NA | 0.07 | 0.07 | 0.05 | 0.06 | ND | ND |
| Healthy donor #5 | NA | NA | NA | 0.05 | 0.05 | 0.05 | 0.06 | ND | ND |
| Healthy donor #6 | NA | NA | NA | 0.05 | 0.05 | 0.04 | 0.07 | ND | ND |
| Healthy donor #7 | NA | NA | NA | 0.05 | 0.05 | 0.06 | 0.06 | ND | ND |
| Healthy donor #8 | NA | NA | NA | 0.05 | 0.05 | 0.06 | 0.07 | ND | ND |

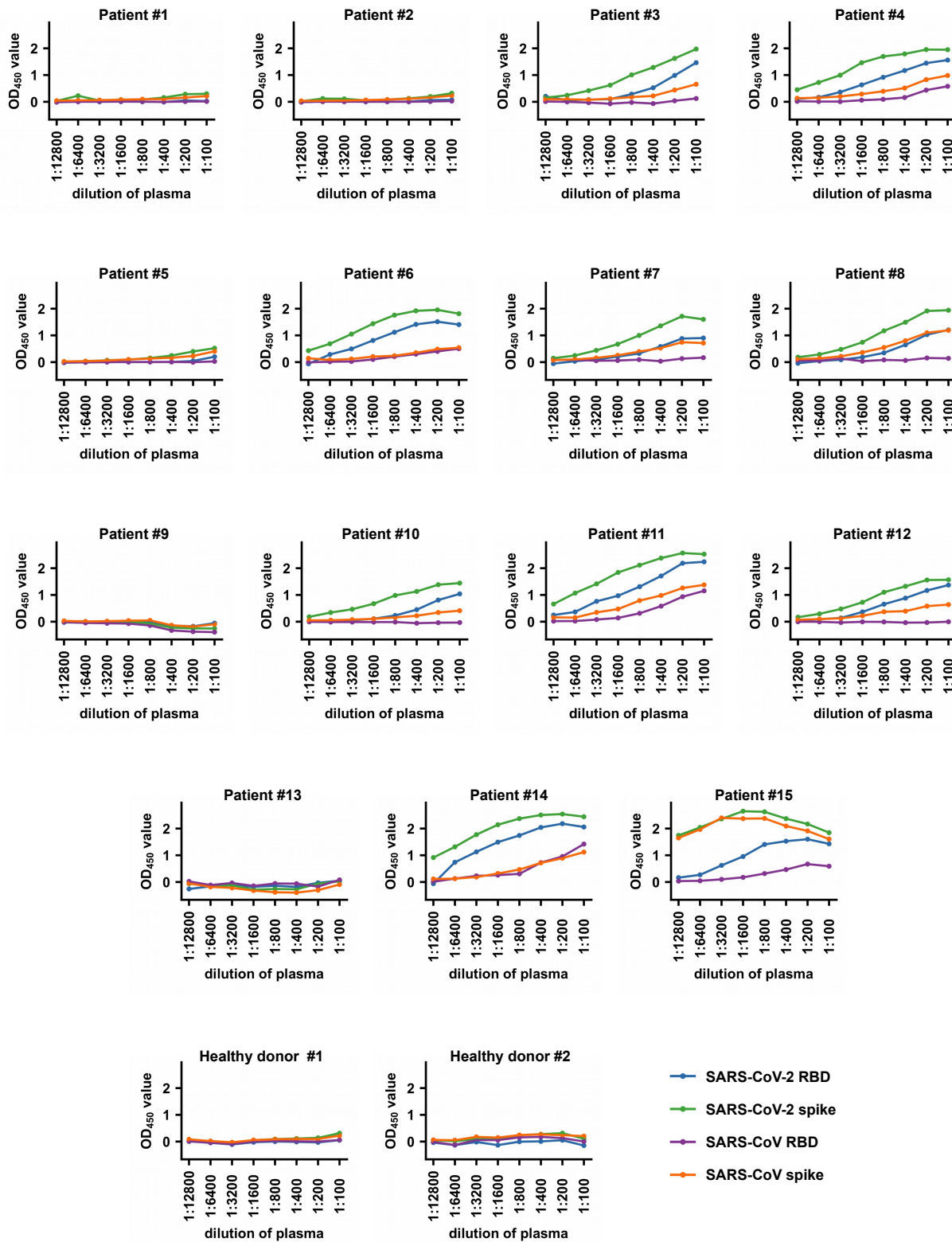NA = Not available/applicable

ND = Not determined

**Figure S1. ELISA of patient samples at different dilutions. Related to Figure 1.** Binding of different dilutions of plasma samples from 15 patients and 2 healthy donors to spike and RBD from SARS-CoV-2 and SARS-CoV was measured by ELISA. The mean $OD_{450}$ values calculated after testing each plasma sample in duplicate are shown.
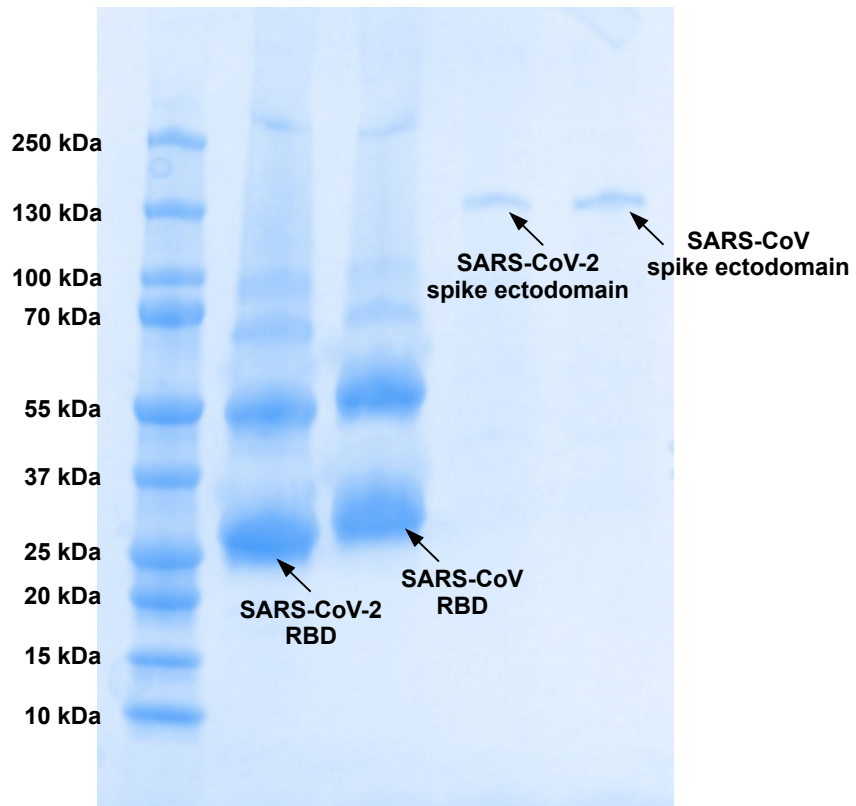
**Figure S2. Protein expression. Related to Figure 1.** SARS-CoV-2 and SARS-CoV ectodomain and RBD proteins were purified by Ni-NTA beads from insect cell expression supernatant and analyzed by Coomassie staining on an SDS-PAGE gel. The proteins were further purified by size exclusion chromatography before use.